ELSEVIER

Contents lists available at ScienceDirect

Energy Reports

journal homepage: www.elsevier.com/locate/egyr



Research Paper

Comparative capacities of residential solar thermal systems versus F-chart model predictions and economic potential in an equatorial-latitude country



Esteban Zalamea-León ^{a,*}, Mateo Astudillo-Flores ^a, Antonio Barragán-Escandón ^b, Manuel Raúl Peláez-Samaniego ^c

- ^a Facultad de Arquitectura y Urbanismo, Universidad de Cuenca, Av 12 de Abril y Agustin Cueva, Cuenca, Ecuador
- ^b Grupo de Investigación en Energía, Universidad Politécnica Salesiana, Calle Vieja 12-30 y Elia Liut, Cuenca, Ecuador
- ^c Departamento de Química Aplicada y Sistemas de Producción, Facultad de Ciencias Químicas, Universidad de Cuenca, Ecuador

ARTICLE INFO

Article history: Received 17 March 2023 Received in revised form 7 September 2023 Accepted 9 September 2023 Available online 18 September 2023

Keywords: Solar thermal Flat plate collectors Evacuated tube collectors Solar thermal performance Residential hot water

ABSTRACT

One popular simulation tool for predicting solar thermal (ST) performance is the F-chart model, which has not been validated for the conditions in equatorial-climate countries. In this work, the performance of two ST systems (evacuated tube collectors (ETCs) and flat plate collectors (FPCs), widely used for supplying domestic hot water (DHW) was assessed and compared with F-chart simulation results. The energy demands were simulated by scheduling hot water discharges and measuring the backup energy requirements to fulfil DHW needs. Then, the difference between the calculated solar fraction using the F-chart model and the measured solar fraction was obtained. Both the measurements and simulations showed that the ETC systems performed better than the FPC systems in a city located on the Ecuadorian highlands with distinct climate conditions. The results showed that ETC systems are, on average, up to 18.5% more efficient than FPC systems. A comparative economic analysis was carried out considering that domestic water heating systems are backed up with liquified petroleum gas (LPG) or electricity, both with and without state subsidies. However, due to the higher cost of ETC technology compared to FPC technology, and despite ETC's higher efficiency than FPC's, only US\$0.34 per month can be saved on average because of the impact of energy subsidies. Thus, the FPC technology seems more profitable, under the mentioned conditions, because of its lower capital costs. With backup systems powered by unsubsidized energy, the two technologies are nearly comparable. The ETC technology appears suitable only under the unsubsidized electricity scenario. The novelty of this research is that real ST systems installed under similar conditions are integrated, the operation of ST technologies for DWH is simulated, and the different inclinations and orientations of solar collectors are considered. The results are compared with simulations from the F-chart model, and each system is economically assessed.

© 2023 The Authors. Published by Elsevier Ltd. This is an open access article under the CC BY license (http://creativecommons.org/licenses/by/4.0/).

1. Introduction

Solar radiation is more abundant than any other renewable energy source on Earth. The solar radiation incidence on the Earth's surface for less than one hour is enough to meet the energy demand of our planet for an entire year (Perez and Perez, 2009). Additionally, the amount of solar irradiation at the Earth's surface could meet the total energy demand of the planet almost 7000 times (The World Counts, 2023). The urban population is expected to reach ~2.5 billion inhabitants by 2050 (United Nations, Department of Economic and Social Affairs, 2018), with additional

energy requirements projected. Addressing the energy crisis will require the use of alternative sources as well as traditional energy resources, which will cause economic and political tensions that lead to conflicts at the local or international level (Astrov et al., 2022). One alternative is to promote and evaluate the capacities of different sources of renewable energy in cities and in buildings under a model of maximum self-supply (International Renewable Energy Agency (IRENA), 2021). Each residential core, including people obtaining their own clean energy, would contribute to energy sustainability.

Solar thermal (ST) technology is an important alternative that has long been used to meet energy demands in buildings. The Solar Heating and Cooling Program of the International Energy Agency (IEA and SHC, 2022) estimated that in 2019, 684 million

^{*} Corresponding author. E-mail address: esteban.zalamea@ucuenca.edu.ec (E. Zalamea-León).

- 1	N.	^	m	An	c	3	***	re

FPC Flat Plate Collector ETC Evacuated Tube Collector

ST Solar Thermal
DHW Domestic Hot Water
PV Photovoltaic

RTD Resistance Temperature Detector f_{real} Real Solar Fraction contributed by the

System

LPG Liquified Petroleum Gas f_{cal} Calculated Solar Fraction

n Number of Days Q_u Useful Energy Q_a Calculated Heat Load

m Mass Flow

Cp Specific Heat Capacity of Water

A Collector Area
I Solar Irradiance
dt Integration Time

C Daily Water Consumption

Tank Water Accumulation Temperature

T_{network} Network Water Temperature

RAD Solar Irradiance

ETC_{Nor} North-Facing Evacuated Tube Collector South-Facing Evacuated Tube Collector ETC_{Sou} ETC_{Fas} East-Facing Evacuated Tube Collector West-Facing Evacuated Tube Collector **ETC**_{Wes} North-Facing Flat Plate Collector FPC_{Nor} South-Facing Flat Plate Collector FPC_{Sou} East-Facing Flat Plate Collector FPC_{Fas} West-Facing Flat Plate Collector **FPC**_{Wes}

 f_{real}/f_{cal} Real Solar Fraction to Calculated Solar

eta Fraction Relation eta Collector Inclination

m² of ST collector surfaces were installed worldwide, with the capacity to prevent 135.1 million tons of CO₂ from entering the atmosphere (Weiss and Spörk-Dür, 2019). The principle of the greenhouse effect and the solar box or thermal concentration irradiated by the sun have been applied to buildings with patent registrations since the 19th century (Morse, 1881), and there are records of the sun being considered in architectural designs since classical times (Vázquez Espí, 1999). The usefulness of ST systems depends on the availability of solar radiation and the conditions influencing demand and the levels of captured radiation can be improved by suitably arranging the collectors and adjusting the storage conditions and capacity (Gajbert, 2008).

ST technology comprises different systems, depending on the constituent materials and configuration of the collection surface. Kalogirou extensively described the capabilities, potential, and limitations of diverse ST technologies (Kalogirou, 2004). The adoption of a specific technology is based on the capacity, technical potential, and/or cost. For buildings, ST is typically utilized to meet domestic hot water (DHW) demand and, to a lesser extent, for heating, recreation, agricultural or industrial uses. For space heating, there is a reduced capacity since in places where and at times when the demand is high, solar irradiance levels are typically minimal; therefore, DHW has been the prevailing application of ST worldwide. The two technologies with the greatest integrability in buildings are evacuated tube collectors (ETCs) and

flat plate collectors (FPCs) (Munari, 2009). FPCs include a flat. metallic absorbent layer under a glazed surface enclosed into an isolated box that provides a low-heat-energy-transfer enclosure with a heat exchanger coil. FPCs exploit all the radiation that reaches the collection surface; however, there are losses due to convection and transmission effects (despite the adoption of glass barriers and isolation measures), which reduce the performance under cold and windy weather conditions. Nevertheless, they are efficient in hot climates and in places with high levels of direct irradiation exposure. ETC technology employs smaller section collectors enclosed in a vacuum environment within glass tubes. This vacuum environment creates isolation, which reduces convection and conduction losses that negatively affect the efficiency of FPCs. Therefore, ETC technology is more isolated than FPC for better performance in cold, windy weather conditions and in cases with diffuse solar irradiance, even though a portion of the radiation is lost since it passes between the tubes (Moldovan et al., 2020).

To implement ST systems, it is important to understand the behaviour of the complete system under specific climate conditions; consequently, performance prediction models of ST technology have been developed. The F-chart model developed by Beckman et al. (1977) is a mathematical method (static model type) that enables thermal supply capacity estimation from the solar source. This model can be applied to estimate ST-based residential hot water consumption. It is a widely used prediction tool that is based on the available irradiation data, equipment specifications, and collection surface information. The model considers the loss coefficient of the product (given by the performance of the ETCs or FPCs), weather conditions, temperature of the supply water building network, storage capacity, foreseeable demand and angle of solar incidence. However, as for any simulation model, the modelled results may differ from actual observations because it is difficult to consider all possible parameters, as noted by Okafor and Akubue (2012).

The proper introduction of a technology for energy supply requires reliable information on the capacity of the system, which requires monitoring and analyses of the real performance of equipment. In Ecuador, alternatives are sought to reduce fossil fuel consumption and mitigate the high negative economic and environmental impacts of subsidies for fuels. Therefore, the main strategy is to reduce state spending on hydrocarbon imports and, in turn, invest in the national clean technology industry (Creamer-Guillen and Becerra-Robalino, 2016), contributing additionally to the promotion of local employment, as discussed by IRENA and ILO (2021).

In this study, the behaviour and capacities of the two described ST technologies (ETCs and FPCs) are assessed in Andean equatorial climatic conditions in the city of Cuenca, Ecuador. The experimental setup for the study is located at 2°54′2.32″S and 79°0′39.44″W. A satellite image of the collectors can be seen in Fig. 1 (using the Google Earth Pro platform). The study location has a particular and relatively stable climate with a solar path that is nearly perpendicular to the ground at noon throughout the year. Due to the mountainous surroundings, the cloud cover is high, but there are also several days with high levels of radiation throughout the year, and the radiation levels vary slightly by season. Thus, the conditions in Cuenca represent the climate conditions of other cities in the South American Andes, as described in a previous study (Zalamea-león and Barragán-escandón, 2021). Due to the locations and climate characteristics of these cities, it is difficult to predict which of the two mentioned ST technologies are more appropriate for residential use. Thus, a comparative analysis between the two technologies in different scenarios is carried out in this study.

Additionally, the differences between the F-chart model simulation results and the real capacity of the technology are explored



Fig. 1. Satellite image of test benches for solar thermal systems observed using Google Earth Pro.

by comparing the simulation results with real performance readings (under the same conditions). Four ST systems were built with two ETCs and two FPCs and, in each system, the collectors were set at different orientations and inclinations, simulating possible arrangements when installed on sloped roofs. It has been established that when photovoltaic (PV) collectors are placed in different orientations and with a low inclination relative to the horizontal axis, the incidence of irradiation is not significantly reduced at the studied latitude (Izquierdo-torres et al., 2019). However, greater inclinations deserve further analysis. Although previous studies analysed the capacity of ST systems, in this work, simulations are conducted using data obtained from real equipment under different working conditions that were monitored daily. The novelty of this work lies in the comparative analysis of the solar systems of two well-known ST technologies in complete installations, including an integrated water storage system and a recirculation system. In addition, the theoretical performance of the F-chart model is assessed based on experimental results, and such an analysis has not been reported previously, according to our literature review.

1.1. Background research

Residential water supply applications of ST technology have been recorded since the end of the 19th century with the "Climax" solar water heater in the United States and subsequent developments in Spain and Cuba, according to Vázquez Espí (1999) and Kalogirou (2004). As early as 1989, in the first description of the capacities of the FPC and ETC technologies, Duffie (one of the main developers of the F-chart model), described the uses and capacities of ST technology. The losses in the ETCs were described as "a quarter, giving more energy, higher temperature, and operating at lower levels of radiation" when compared to those observed in FPCs [18]. Performance prediction models for ST technology were published as early as 1988, such as by Prapas et al. (1988). Subsequently, the authors began to analyse the capacity of ST technology with collectors arranged in different orientations and inclinations to determine the best deployment of an ST system according to location and use. The authors also

found that in Malaysia, up to 40% more radiant power can be received over one year by adjusting the inclination of the collectors (Bari, 2000). Interestingly, to the best of the authors knowledge, no have reported the influence of collector inclinations on the radiant power received under the conditions in equatorial cities at high altitudes, as those in the Andean highlands.

Recent research for improving the thermal performance of ST collectors has focused on studying how a specific technology, under different climate and solar conditions, could increase their capability. Singh and Das (2022), for example, analysed the performance of different air conditioning systems that operate with ST energy, considering refrigerant flow variability and inclination, and their performance was compared with that of conventional air systems. The authors found that better air conditioning performance results are obtained with variable refrigerant flow, reaching an energy efficiency improvement of up to 23% depending on the climate conditions and air humidity variations. However, the study was performed with simulations and climate data available in commercial software but not with real onsite performance measurements. Another study performed by the same authors determined the efficiency of hybrid systems for energizing air conditioning systems with ST, biomass, and an electrical generator. In the work, the authors compared simulations with real data from specific experimental systems for validation. Additionally, the payback period was noted as an important factor related to the viability of an ST project (Singh and Das, 2021).

In another study, a comparative analysis of FPC and ETC technologies was performed, and the effect of vacuum tubes blocking each other in vertically arranged collectors was assessed (Shah and Furbo, 2004). The authors observed that to achieve better performance, the distance between the central axes of vacuum tubes with a diameter of 4.7 cm must be at least 20 cm to reduce the effect of inter shading between the tubes. In another comparative study of the performance of ETCs and FPCs (Zambolin and Del Col, 2010), the difference in efficiency between the two collector types was established. ETCs were found to be more efficient in cold and low-irradiation conditions, whereas FPCs performed better under high direct solar irradiation conditions.

A whole system prediction model with the F-chart model was developed by Klein, Beckman and Duffie in 1976 (Klein et al., 1976). It is a widely applied model for the prediction of ST performance and has been disseminated as an easily programmable tool in an electronic datasheet and freely distributed by state entities that seek to expand the use of ST technology (Minenergia, 2022). This model has been recommended as a predictive tool in Ecuador for evaluating the performance of ST technologies (Obaco and Jaramillo, 2010) and has been compared with complex dynamic models. The comparison showed relatively similar results, with lags of up to 5% (Dongellini et al., 2015; Guilló et al., 2008), which is in the error range of simulations.

Previously, the application of the F-chart model to the collector arrangements in the study region was analysed through this method, and the capacities of ETCs and FPCs with different inclinations and orientations were compared. It has been estimated that the greatest capacity is realized when the collectors are arranged with an inclination close to the horizontal axis and oriented south, which contradicts the theoretical performance results in principle, since if the latitude of the collector location is the Southern Hemisphere (2, 54° south), as a rule, the best orientation is north. However, in the study location near the equator, there is a high incidence of cloudiness in the summer season in the Northern Hemisphere. It has also been previously determined that ETC technology theoretically outperforms FPC technology in the region by up to 26% of the solar fraction when applying the F-chart (Astudillo-flores et al., 2021). However, for PV technology, it has been established that in Cuenca, the PV performance is better with an east orientation (with an inclination of 14°), namely, the performance is 7.05% better than when the PV faces west with a 26° inclination, and if they are on the same incline, the performance is improved by less than 1%. This result is a consequence of the lower cloudiness in the morning, but it is concluded that any orientation is adequate when the PVs are arranged with a low slope. However, in the same study, it was concluded that increasing the slope is appropriate to keep the PV clean, given the high levels of rainfall, with losses of less than 3% due to natural cleansing from the rain (Izquierdo-torres et al., 2019).

Studies have also been performed to evaluate the real performance of ST output compared with the real output per example in the study performed by Zhang et al. (2021) for PV-ST solar plates. Additionally, in Ecuador, the performance of a single ETC has been determined by establishing the thermal output, as in the study performed by Recalde et al. (2015), among the studies detecting collector performance. The work presented herein seeks to advance our understanding of the performance of complete and real-scale residential ST systems considering storage, real climate conditions, and the thermal distribution. Therefore, the true performance of ST systems is assessed when deploying collectors for irradiation capture at different orientations and inclinations representative of the slopes of roofs in Latin America and the Andean region, representing the situation of collectors placed in a coplanar layout with respect to inclined roofs. This study complements a previous study in which the incidence of shadows of evacuated tubes compared to those of FPCs and the performance of solar thermal systems were analysed (Zalamea-Leon et al., 2021).

2. Methodology

To determine the capacity and efficiency of both technologies and to identify the solar fraction, it is necessary to measure the level of irradiation at the moment of generation and determine the proportion of energy used. In addition, other air and water temperature parameters are needed. To collect data

Table 1Evacuation volumes and discharge times of the four solar thermal systems.

Schedule/Collector	ETC02	ETC01	FPC02	FPC01	Evacuation volume (L)
Morning 1 Shower	06:00	06:05	06:10	06:15	52
Morning 2 Sinks	06:55	07:00	07:05	07:10	20
Morning 3 Dishwasher	07:50	07:55	08:00	08:05	8
Afternoon 1 Kitchen	12:00	12:15	12:30	12:45	16
Afternoon 2 Baths	13:15	13:30	13:45	14:00	16
Night 1 Kitchen	19:00	19:05	19:10	19:15	16
Night 2 Baths	19:55	20:00	20:05	20:10	20
Night 3 Shower	20:50	20:55	21:00	21:05	52

on solar radiation and ambient temperature, the Delta T model GP2 weather station is used (Delta-T devices, 2019). The data sampling period is calibrated with a resolution of 10 min, which enables momentary climatic and cloud variation detection. To determine the capacity of the ST technology, four individual systems are deployed in complete residential kits. The four systems are decoupled with the collectors separated from the isolated storage tank, which is an appropriate configuration for architectural and aesthetic integration and for lower seismic risk. The FPC-type ST systems are integrated with 200 litre storage, and the ETC systems are integrated with 300 litre storage, which is the recommended volume for residential kits. The ETCs use the Apricus ETC20 model (Apricus, 2021) with 20 evacuated tubes, with a total surface area of 3 m² and a net collecting area in the tubes of 2 m², according to the technical specifications. The FPC systems use the Shanghai APS Eco-tech CO model (APS Products, 2020). The temperature is measured using resistance temperature detector (RTD) PT100 Autonics thermocouples (Autonic, 2021) placed inside the thermotanks and RTD PT1000 thermocouples at the outlets of the collectors. Fig. 2 shows the connection diagrams for both types of domestic hot water, as well as the locations of the thermocouple sensors and photographs of the four collectors and storage systems. The installation cost of each FPC system is US\$887.50, and that of each ETC system is US\$1425.00; thus, the second technology has a 60% higher cost.

To simulate the operation of each of the systems under the residential use scenario, water is automatically evacuated to reflect residential use, as characterized in a previous local study (Calle-Siguencia and Tinoco-Gómez, 2018). This evacuation is scheduled with an automated system that releases 200 L per day from each water heater at a water temperature that reflects potential residential use, with higher scheduled discharges in the morning and at the end of the afternoon and two smaller discharges at midday. The water temperature is measured at the outlet of the water heaters to discern the temperature needed to reach the 50 °C minimum required at the time of discharge in the respective volume. The evacuated volumes and discharge times are the same among the four systems but with a 5-minute delay to avoid coinciding flows since the pipes lead to a single pipe that carries hot water to the university pool. The evacuations are described in Table 1.

Each system is connected to an SR658 controller (Hetzonneboilerhuis, 2015), which has a data logger and is in charge of measuring and storing the temperature data for each of the zones of the system. This equipment is calibrated with the same sampling frequency as the weather station.

2.1. Variable parameters

For the parameters to be modified, under the limitation of having four complete residential systems (two of each type and for a limited time), performance measurements can be made for periods of at least three weeks. The ideal period for each deposition would be an entire year, but a shorter period is also valid

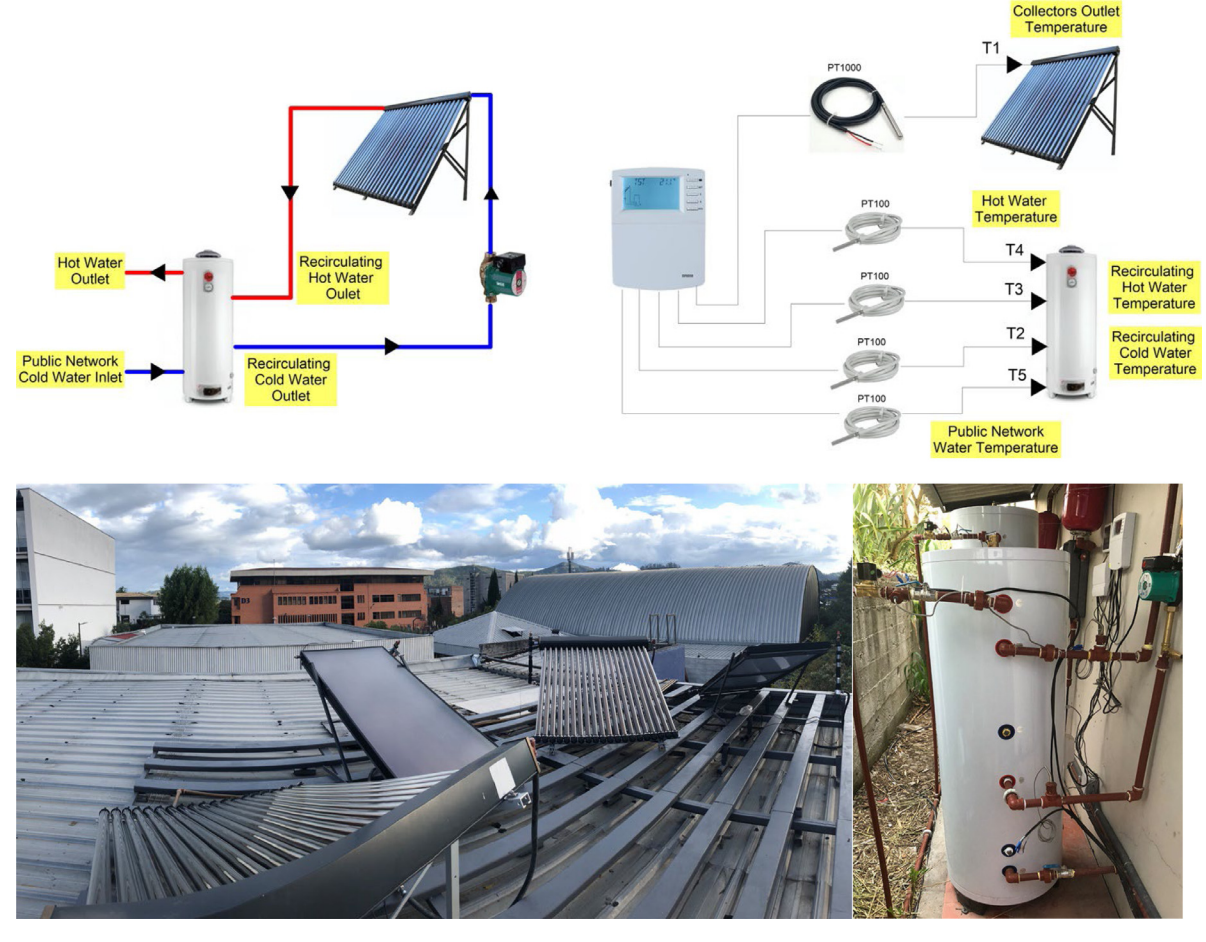


Fig. 2. Solar collector connection diagram and installation photos.

for the established goals since the comparison of performance between both technologies is performed, especially under climate conditions with minimum seasonal influence. Additionally, a comparison with the F-chart model is also possible, since in the model, the irradiation availability data are taken on-site, and the angular incidence obtained when the thermal output is taken is also considered as input data in the model. The measurements were taken from May 2020 to February 2021. The slopes of the collectors are typical for local roofs, namely, 14°, which reflects the slope of fibre cement roofs and arrangement in flat roofs; 18°, corresponding to the slope of traditional tile roofs; and 26° and 45°, corresponding to 50% and 100% of the slope, respectively, representative of roofs of maximum slope observed locally, normally used to create interior spaces of habitable rooftops. The orientations considered for analysing the heating potential of the DHW are the four cardinal directions. At equatorial latitudes, solar incidences in the four orientations are high if the slope of the collectors is low in the annual balance, which implies that the orientation does not greatly influence the total energy collected but does influence the hours of capture and the amount of overlap between hours of use (Mulcué-Nieto and Mora-López, 2017), thereby affecting the obtained caloric energy. The inclinations and orientations of the solar collectors were varied according to Table 2.

Based on the collected data, with the irradiation levels and temperatures obtained in different positions in the ST system (T_n) , we calculate the solar fraction contributed by the ST systems (f_{real}) . Likewise, the energies required by an auxiliary electrical system and by liquified petroleum gas (LPG) combustion to reach the required water temperature are also determined.

Table 2Data collection dates for the solar collectors.

Data concerion dates for the solar concerors.								
Data collection date	Inclination	Orientation						
03 May-27 Jun	14°	-FPC oriented east-north						
01 Aug-02 Sep	45°	-ETC oriented west-south						
03 Sep-24 Sep	26°							
25 Sep-21 Nov	18°							
Change in orientation								
29 Nov-17 Dec	14°	-FPC oriented west-south						
18 Dec-07 Jan	18°	-ETC oriented east-north						
08 Jan-24 Jan	26°							
25 Jan-21 Feb	45°							

Next, once climatic information is collected and the performance of the collectors is evaluated, the solar fraction is calculated via the F-chart method (f_{cal} in our calculation). The calculation of the solar fraction is performed according to the method described by Klein et al. (1976), and their equations and mathematical development were presented in detail in a previous study (Astudillo-flores et al., 2021).

In this study, however, the performance is estimated based on the irradiation available over three weeks for each of the collector arrangements, which is then extrapolated to the corresponding month, that is, with a minimum reading sample of 67%, considering the solar path corresponding to that period. This information is required to calibrate the F-chart. Importantly, in this case, the model is applied in two different stages. In the first stage, the average radiation is used during the number of days (*n*) that data were collected for the inclinations and orientations shown in

Table 1. In the second stage, only the data for the day of maximum radiation are used, and with n equal to the number of days, data were collected for each inclination and orientation.

To calculate the real solar fraction (called f_{real}), the methodology described by Obaco and Jaramillo is used (Obaco and Jaramillo, 2010) based on a model originally proposed by Klein and others (Klein et al., 1976), where f_{real} is the ratio between the useful energy (Q_u) collected by the collector and the calculated heat load (Q_a) .

$$f_{real} = \frac{Q_u}{Q_a} \text{ (Klein et al., 1976)} \tag{1}$$

The useful energy collected by the collector, in our case, is defined by the following formula.

$$Q_{u} = \frac{\int \dot{m} \times Cp \times (Toutlet - Tinlet) \times dt}{A \times \int I \times dt} \text{ (Klein et al., 1976)} \quad (2)$$

where

 \dot{m} , is the mass flow that circulates through the system (0.22 kg/s), Cp is the specific heat of water (4187 J/kg $^{\circ}$ C),

A is the area of the collector,

I is the solar irradiance (W/m²), and

dt is the integration time.

The heat load is calculated by the following formula.

$$Q_a = C \times Cp \times n \times (Taccumulation - Tnetwork)$$
 (Klein et al., 1976)

(3)

C is the daily water consumption (I/day), Cp is the specific heat of water (4187 J/kg $^{\circ}$ C), n is the number of days that samples were taken, $T_{accumulation}$ is the accumulation temperature of the tank, and $T_{network}$ is the water temperature of the network.

3. Results

3.1. ST performance under varied inclination and orientation settings

The result sought in this work is the temperature of the outflow of each storage thermotank, which reflects the usable thermal energy for consumption and therefore can be used to determine the backup power required and real ST capacity. The first observable result is the direct correlation between the temperature reached and the level of solar irradiance. Next, the average temperature curves in each of the ST systems at the T4 output are calculated for 32 scenarios (north, south, east, and west orientations, in four inclinations and two technologies), as shown in Fig. 3 from (a) to (h). These temperature curves are compared with the global average solar irradiance curves measured on the same days. The ideal scenario would undoubtedly be to obtain these curves under levels of identical irradiance for all circumstances; however, doing so would require many systems to be installed simultaneously in the laboratory. Beyond this, the objective of this work is to determine the reliability of the simulations and the performance of the complete systems at the hot water outlet. In the subsequent figures, the red-marked lines correspond to irradiation and temperature when the collectors are deployed at a 14° tilt, with blue-marked lines denote when the collectors are deployed at a 18° tilt, yellow lines when they are set at a 26° tilt and green lines when they are set at a 45° tilt. When the collector's tilt increases, theoretically poorer performance would be expected, since the radiation incidence on average becomes more tangential in equatorial regions.

As expected, the temperature measurement results indicate that the maximum temperatures of the curves are a consequence of higher levels of solar irradiance. It is also observed that the trend exists minimally at higher temperatures with the collectors deployed with lower slopes, although not significantly as expected. The maximum temperatures reached under the proposed inclinations in both technologies are not very different, namely, 32.4 °C in the ETC system inclined 14° and oriented north and 26.7 °C in the FPC system oriented north and inclined 26°. The time at which the temperature is the highest when leaving the storage tanks in all cases is 15:00 to 16:00. The trend also indicates that in general, the systems heated by the ETCs tend to reach higher temperatures; however, when the FPCs are under greater solar irradiance, the average temperatures reached for the FPC systems are even higher than those reached by the ETCs (in the case of the ETC and FPC systems) at the T4 outlets of the storage tanks.

The most important performance difference between the ETC and FPC systems is the significant and rapid temperature reduction in the thermotanks, especially those caused by the nocturnal discharges that simulate the night consumption under the scenario described in Table 1. Three consecutive discharges of a total of 88 L are scheduled in each system, which implies that the temperature of the FPC systems is reduced between 7 °C and 9 °C, whereas that of the ETC systems is only reduced between 1 °C and 4 °C in the outlets of the thermotanks. This is a logical and consequential aspect of the different storage volumes and therefore the lower thermal energy contained (200 L vs. 300 L). This finding implies that for calculating the energy needed for the discharges scheduled in the morning, the required backup temperature is higher in the systems supplied by FPCs, and therefore, the energy consumption is higher. This result is also consistent with the results of a previous study carried out on these same specimens, where it was determined that in the case of the two technologies deployed at the same inclination (14°), the FPC systems require between 21% and 17% more backup power than the ETC systems (Zalamea-Leon et al., 2021); therefore, the best ETC capacity is in moderately cloudy and highly cloudy scenarios.

3.2. Computation and comparison of f_{real} and f_{cal}

freal (the water heating and solar fraction in real measurements) is measured by applying model (1), considering the temperature at the outlets of the tanks and the variation in this temperature in each discharge and by thermal losses from the system. It is analysed for a temperature requirement of at least 50 °C in each of the consumption flows according to the standard (Ministerio de Desarrollo Urbano y Vivienda, 2020). Table 1 shows the calculated complementary energy demand and therefore the average solar contribution on the days in which the measurements were made. Then, through the F-chart model, in accordance with the period of the year and the solar angle on the collectors coinciding with the date of taking real measurements. the model is calibrated with the onsite level of solar irradiance, ambient temperature and water temperature. When evaluating the performance of the ETCs from the F-chart model, the solar fractions f_{real} and f_{cal} are compared, and the results are presented in Table 3 for the ETC technology and in Table 4 for the FPC technology.

Tables 3 and 4 also present the average daily solar irradiance scenarios in which both solar fractions f_{real} and f_{cal} were determined based on each collector arrangement, which affects water heating. The indicator f_{real}/f_{cal} is also presented as a percentage, which is used to compare the variation in the solar fractions obtained in different collector arrangements and the percentage variation in efficiency in accordance with the data detected in each system versus the theoretical fraction. The third aspect shown in the tables is the percentage variation in efficiency of

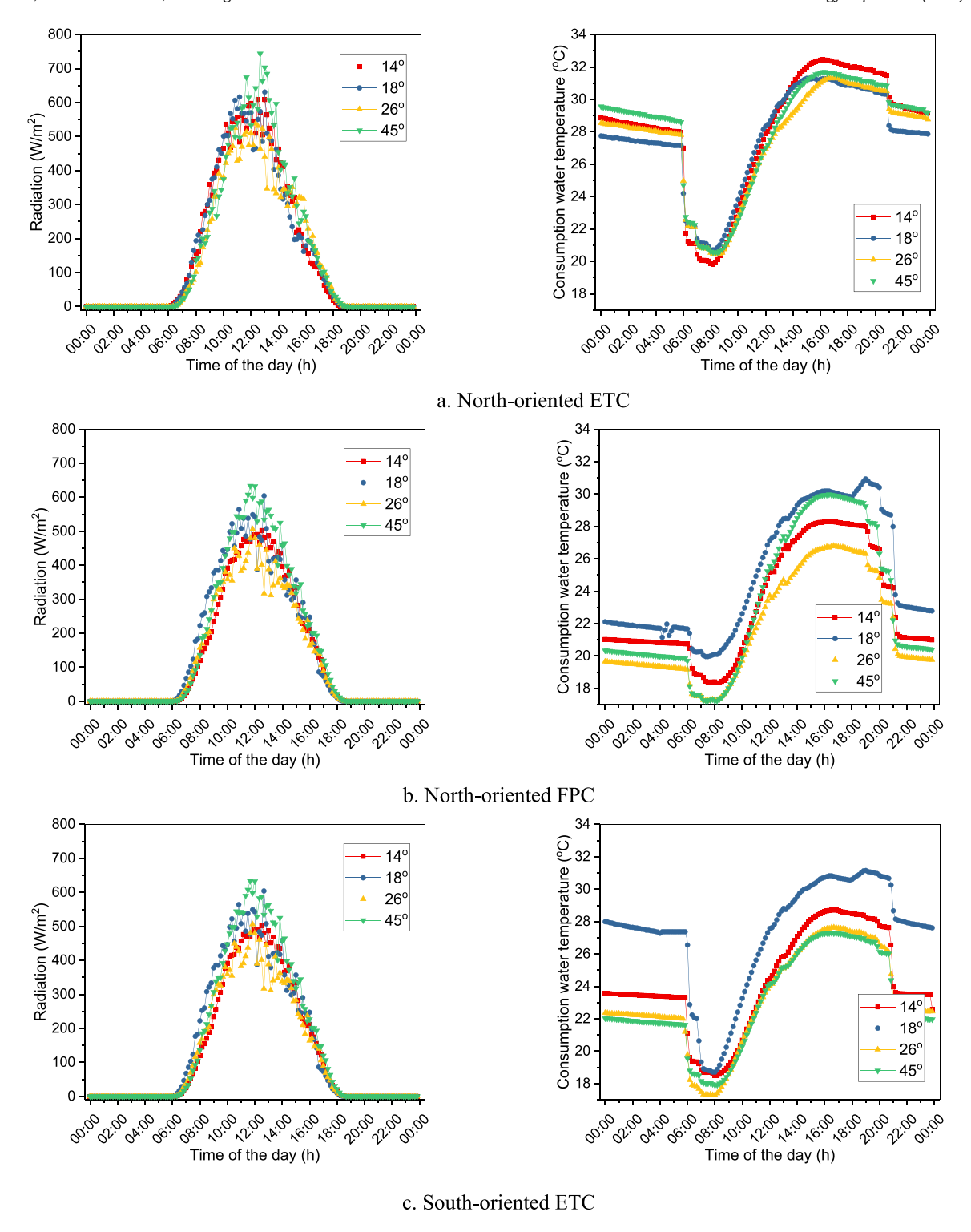
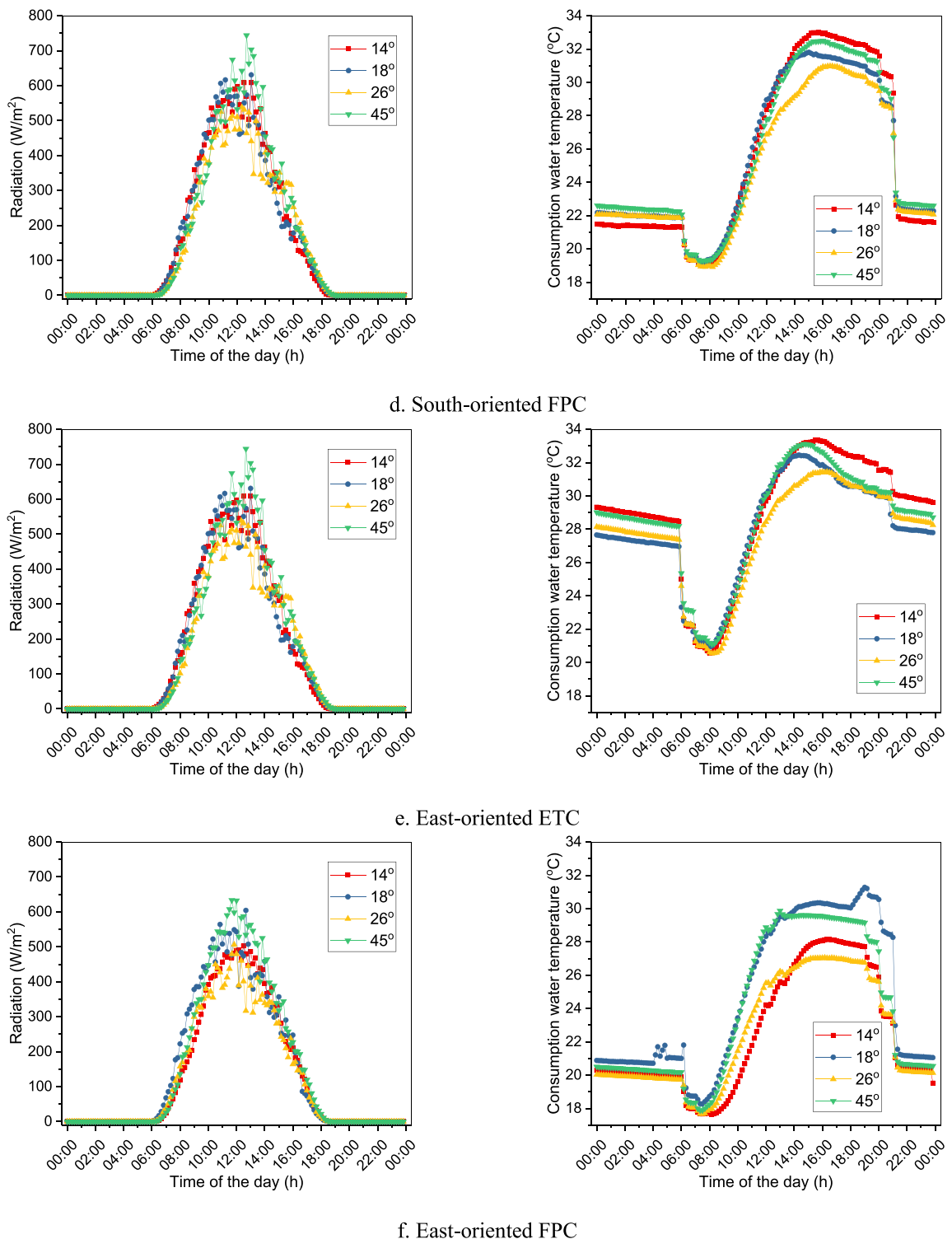


Fig. 3. Readings of the hourly average irradiation and average consumption water temperatures measured at the outlets of the ST collectors. (For interpretation of the references to colour in this figure legend, the reader is referred to the web version of this article.)

each incline of the collector with respect to the previous, less steep incline. One of the most important aspects observed in Table 2 is the comparison of the real fraction f_{real} of the system among different inclination scenarios, which is the minimum loss due to the increase in inclination (between 0% and close to 6% in situations of similar irradiance). However, important reductions are detected when the solar irradiance is significantly reduced; for example, in the case of the west orientation, by increasing the inclination between 18° and 26°, f_{real} is reduced by 19.18 points of

this fraction index. Regardless, when the average daily irradiance increases, between the inclinations of 26° and 45° , the solar fraction increases by 18.85%, contrary to expectations. For the north orientation, we see, for example, that with an inclination of 45° , the solar fraction exceeds that in the 18° inclination scenario (57.7 versus 56.7) and is much greater than that with an inclination of 26° . This result is also due to the higher levels of direct solar irradiance, especially in the afternoons when the collectors were tilted at 45° , which produced a higher tank temperature



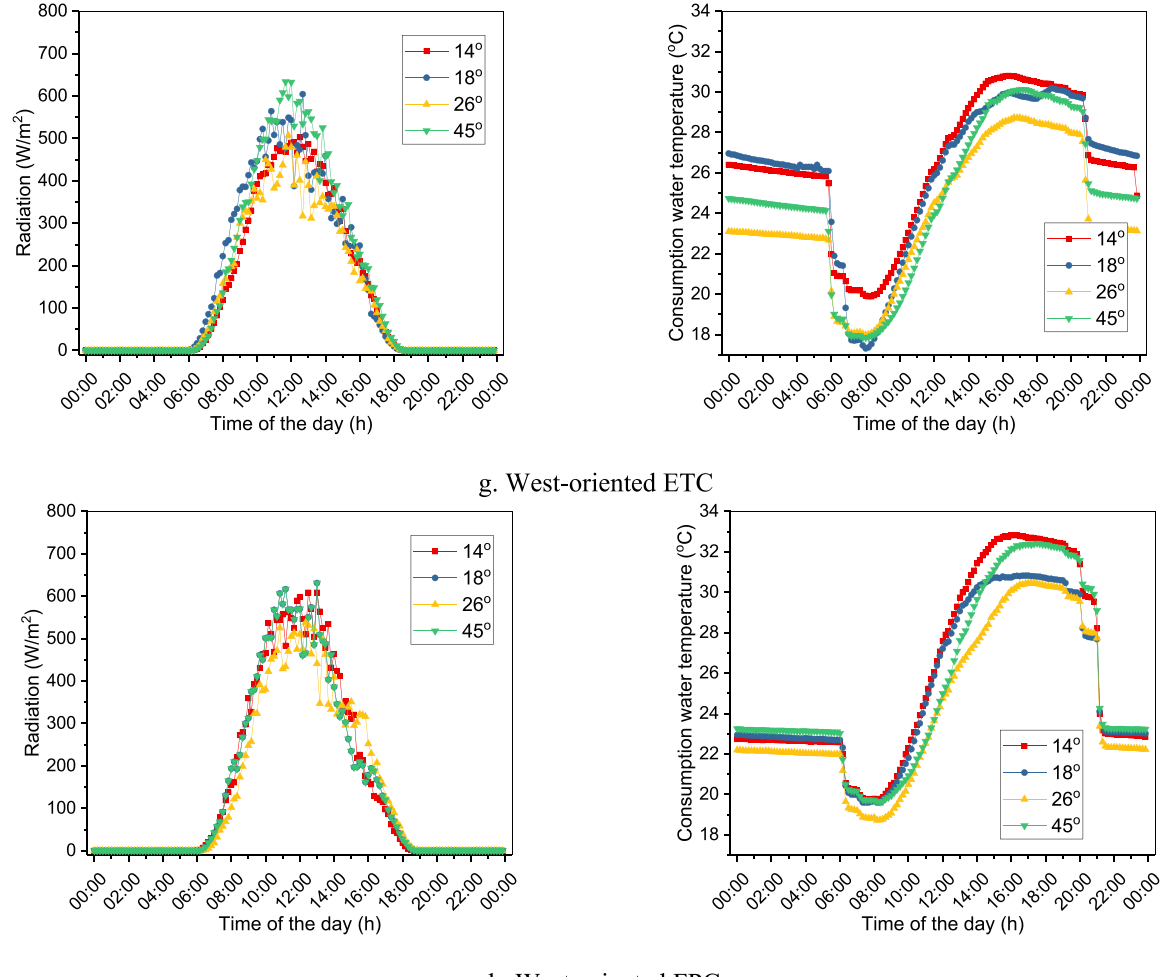
i. Last offented i i C

Fig. 3. (continued).

during the night hours of high discharge. From then on, in the scenarios of the other orientations, a decreasing trend is observed in f_{real} as the collectors are arranged with a greater inclination setting, as expected. The reductions typically observed due to the increasing inclination of the collectors, however, are less than those obtained for the theoretically calculated fraction f_{cal} . Table 3 shows f_{real} and f_{cal} , along with the percentage efficiency reduction that occurs as the inclination increases, highlighted in green,

and the exceptions where the efficiency increases despite the increasing inclination highlighted in orange, which is visualized with respect to the higher solar irradiance levels expressed in RAD Wh/m^2 day parameter.

For the ST installations powered by FPCs, the same comparative procedure is carried out, and the maximum real solar fraction f_{real} reached is 37.4 with the collector arranged at a 14° inclination and oriented to the east. This finding is similar to



h. West-oriented FPC

Fig. 3. (continued).

studies that demonstrate the same pattern locally for PV, namely, that the eastern orientation is the most favourable (Izquierdotorres et al., 2019). In contrast, the lowest f_{real} detected is 25.0, which occurs with the FPCs oriented to the north at an inclination of 26° . This occurs when there is low average solar irradiance (3065.9 Wh/m²) and during the month of September when the sun no longer travels from the north but passes approximately perpendicularly over the ground at this latitude. Although not linear, there tends to be a lower solar fraction when the collectors are more inclined. However, although f_{real} can be high even on steep slopes under intense average insolation (see Table 4), when the FPCs are oriented northwards, f_{real} increases by 14% as the inclination increases from 26° to 45° because of the increasing average solar irradiance from 3065.9 Wh/m² day to 3847.6 Wh/m² day.

 f_{real} increases even though the theoretical simulations of the F-chart indicate that as the measured solar irradiance grows, the solar fraction should be reduced. Compared f_{cal} with f_{real} in systems powered by FPCs, unlike what is measured and simulated in the ETCs, f_{cal} of the FPCs is higher than f_{real} when the FPCs are arranged at a low inclination, with f_{real} between 79.07% and 98.55% of f_{cal} . However, when the inclination is greater, f_{real} grows comparatively; thus, with an inclination of 45° facing in south, east and west orientations, the indicator f_{real} is 220%, 2%, 182.8% and 358.1% of f_{cal} , respectively. The only exception is with the FPCs oriented to the north and inclined at 45°, where f_{real} is 89.7% of the magnitude of f_{cal} . According to our observations, this result may be due to the effect of the sun's path on insolation

coming from the Northern Hemisphere (between May and June), which is further influenced by the low cloudiness in that period of measurement. However, the trend indicates that in the remaining cases, when the slopes are high, the theoretical performance f_{cal} is significantly reduced, which is not observed for f_{real} , and that with a low inclination (14°), f_{cal} is always higher than f_{real} , with the latter between 79.07% and 98.55% of f_{cal} .

Graphs of f_{real} and f_{cal} are presented in Fig. 4 for the case of FTCs. The trend suggests that the real performance is better than the simulated performance in the 16 cases using this technology. Generally, as the slope increases, the difference between f_{real} and f_{cal} also increases. For f_{cal} in the east and west orientations, the reductions due to greater inclination are considerable and more pronounced than the theoretical reductions expected in the ETCs arranged facing north and south, which are not detected during the measurements made to establish f_{real} (Fig. 4).

When analysing the capabilities of FPC technology, f_{cal} surpasses f_{real} when the collectors are oriented north and south on average, except with high inclinations (26° and 45°) facing south, where FPC f_{real} is greater than f_{cal} . Consequently, the output thermal measurement was obtained when the FPC was facing south, which is when the irradiation comes from the Southern Hemisphere (Jan–Feb). Then, the F-chart model does not express the thermal increase jointly by more direct irradiation and slightly higher climate temperatures in this period. Therefore, with high average solar irradiance and sunshine from the south in December, the month in which the FPCs were monitored, because the solar incidence comes from that orientation, the tendency varies

Table 3 Real and calculated solar fraction and average radiation values for the FTC system. Inclination of ETCs 269 459 149 18° RAD Wh/m2 day 3676.9 3663.7 3767.4 3676.8 -2.74% f_{real} 56.7 54.8 -6.00% 57.7 -1.03% 58.3 NORTH f_{cal} 48.76 46.22 -5.21% 39.89 -13.70% 24.76 -37.93% % freal/fcal 119 57% 137 38% 233 04% 122 67% RAD Wh/m2 day 3550.3 3065.9 3847.6 3134.8 -2.88% f_{real} 59 57.3 51.1 -10.82% 52.2 2.15% SOUTH f_{cal} -18.35% 33.09 29.24 -11.63% 46.22 37.74 -12.32% % freal/fcal 127.65% 151.83% 154.43% 178.52% RAD Wh/m2 day 3676.9 3663.7 3767.4 3676.8 f_{real} 59.9 58.7 -2.00% 58.4 -0.51% 58.8 0.68% EAST f_{cal} 32.05 -34.27% -16.76% 20.61 -22.75% 48.76 26.68 % freal/fcal 122.85% 183.15% 218.89% 432.04% RAD Wh/m2 day 3847.6 3134.8 3550.3 3066.0 f_{real} 55.8 -4.45% 45 1 -19.18% 53.6 18.85% 58.4 WEST 41.43 30.49 -14.33% 21.5 -17.69% -26.41% 26.12 $% f_{real}/f_{cal}$ 140.96% 183.01% 172.66% 249.30%

compared with other north- and south-facing collector results. Then, with the FPCs oriented to the east and west, f_{cal} is higher than f_{real} only when the inclination of the collector is low. As the inclination increases, the trend indicates that f_{real} is minimally reduced because of the slope, but this index is mainly reduced because of reduced average solar irradiance. The nearly linear reduction in f_{cal} as the slope increases in the calculation of the F-chart indicates that under a steep inclination, there is a great difference between the two fractions, with f_{cal} being significantly less than f_{real} (Fig. 5).

3.3. Residential performance and economic implications

A practical approach to identifying the implications of adopting one technology over another under various scenarios for collector arrangements relative to the sky is to determine f_{real} , which establishes the unmet energy requirement for covering DHW, considering the backup energy required from the two typical sources: electricity and LPG. freal is analysed considering the measured monthly cost in each case. For this purpose, the cost of these energy sources is also considered, along with the real cost of energy. Since the high subsidies in Ecuador make any of the alternatives unprofitable, this work seeks to identify a technology to which spending on subsidies can be redirected. A cost of US\$23.03 for a 15 kg LPG commercial tank (15 kg gas tanks are the local subsidized LPG sales mode) is estimated based on the international LPG value as of May 2022 (Petroprices, 2022), whose high price is influenced by the Russia-Ukraine conflict. The price of residential subsidized electricity is close to US\$0.10er kWh hour. However, in 2022, the real price of electricity was approximately US\$0.156 (Agencia de Regulación y Control de la

Electricidad, 2022). The determined monthly costs of different backup energy sources for systems powered by FPC technology and ETC technology are presented in Tables 5 and 6, respectively.

Table 6 shows the energy requirements and the economic expenditures on backup energy for systems powered by ETCs for the cases in which they are powered by subsidized LPG, unsubsidized LPG, subsidized electricity, and unsubsidized electricity.

The results regarding the monthly financial expenditure to feed the backup systems under the proposed cost scenarios demonstrate that in the case of subsidized LPG, the additional energy required to meet the demand in the case of the FPCs ranges from US\$2.13 with the FPCs oriented to the east to US\$1.63 when the FPCs are oriented north and inclined 14°; on average, US\$1.76 per month is required in all the situations analysed. In contrast, for systems powered by ETCs, the cost for backup energy ranges from US\$1.68 with the ETCs oriented south and inclined 26° to at least US\$1.31 with the collectors inclined 14° and oriented north. Overall, for ETC technology, an average of US\$1.42 is required in subsidized backup LPG. Comparing the two technologies, it is inferred that on average, among all the situations, cases and backup energy sources analysed, the cost associated with ETCs is 18.5% lower than the cost of energy using FPC technology. Although the analysis is undoubtedly limited and financial parameters will change over time, it provides an estimate of the LPG cost that can be saved monthly over the 15 years of useful life of the ST systems with actual circumstances, with the difference between these two technologies being US\$46.80 over this long period; this low economic difference is a consequence of the unrealistic prices of energy in Ecuador, which are far from profitable. However, ST systems have been implemented in the country due to environmental awareness above all other motivations. Under

Table 4

Ir	nclination of FPCs	14°		18°		26°		45°	
	RAD kWh/m² day	3134.8	3134.8 3550.3		3	3065.9		3847.6	
NORTH	f_{real}	33.4	34.1	2.1%	25.0	-26.7%	28.5	14.0%	
	$f_{\it cal}$	38.0	40.1	5.6%	34.8	-13.3%	31.7	-8.7%	
	% $f_{\it real}/f_{\it cal}$	88.01%	88.01% 85.1%		71.9%		89.8%		
	RAD kWh/m² day	3676.9	3676.9 3663.7		3767.4		3676.8		
SOUTH	f_{real}	35.7	35.0	-2.0%	33.0	-5.7%	36	9.1%	
	$f_{\it cal}$	45.2	36.8	-18.4%	30.9	-16.2%	16.4	-47.0%	
	% $f_{\it real}/f_{\it cal}$	79.07%	g	95.1%	1	06.9%	2	20.2%	
	RAD kWh/m² day	3134.8	3550.3		3065.9		3847.6		
	f_{real}	37.4	32.1	-14.2%	26.9	-16.2%	31.3	16.4%	
EAST	$f_{\it cal}$	38.0	26.4	-30.4%	21.6	-18.3%	17.1	-20.7%	
	% $f_{\it real}/f_{\it cal}$	98.55%	98.55% 121.5%		124.5%		182.8%		
WEST	RAD kWh/m² day	3676.9	3	663.7	3	3767.4	3	3676.8	
	f_{real}	37.1	34.5	-7.0%	33.8	-2.0%	35.7	5.6%	
	$f_{\it cal}$	45.2	28.8	-36.3%	23.4	-18.8%	10.0	-57.3%	
	% $f_{\it real}/f_{\it cal}$	82.17%	1	20.0%	1	44.8%	3	58.1%	

Table 5Unmet energy requirement – FPCs.

ST collector inclination and orientation	Average monthly unmet energy requirement (kWh)	15 kg LPG tank units required	US\$ in LPG per month (at subsidized value)	US\$ in LPG per month without subsidy (US\$23.03 per cylinder as of May 2022)	US\$ in electricity per month (at subsidized value, US\$0.10)	US\$ in electricity per month (without subsidy US\$0.1559)
14° north	198.427	0.989	1.63	22.13	19.27	30.05
18° north	209.437	1.044	1.70	23.02	20.05	31.26
26° north	251.330	1.253	1.79	24.21	21.09	32.88
45° north	208.857	1.041	1.85	25.04	21.81	34.00
14° south	193.887	0.966	1.68	22.72	19.79	30.86
18° south	196.044	0.977	1.73	23.47	20.44	31.87
26° south	209.313	1.043	1.82	24.59	21.42	33.40
45° south	206.165	1.028	1.72	23.26	20.26	31.58
14° east	192.738	0.961	1.68	22.78	19.84	30.93
18° east	200.493	0.999	1.77	24.04	20.94	32.65
26° east	210.887	1.051	2.13	28.85	25.13	39.18
45° east	218.118	1.087	1.77	23.98	20.89	32.56
14° west	197.928	0.987	1.64	22.26	19.39	30.23
18° west	204.429	1.019	1.66	22.50	19.60	30.56
26° west	214.250	1.068	1.77	24.03	20.93	32.63
45° west	202.590	1.010	1.75	23.67	20.62	32.14
Average per month			1.76	23.78	20.72	32.30

the LPG subsidy removal scenario, the maximum monthly energy requirement for the FPC systems is US\$25.04, and the minimum is US\$22.13, with the average for the analysed cases being US\$23.78. According to the same analysis for ETC technology backed by unsubsidized LPG, the minimum monthly expenditure required for backup water heating is US\$17.81, and the maximum is US\$24.42, with the ETC technology average being US\$19.39 in LPG. Over the 15-year useful life of backup energy, the installation of ETC technology would provide a savings of US\$790.20. The difference in cost between the technologies suggests that ETCs

are more costly for residential installation (US\$537.50 difference) but that over the next 15 years, accounting for a future value increase rate of 3%, FPCs practically pay for themselves over time. If a devaluation rate is added to the increasing cost of LPG in the future, which is expected to exceed 3% per year, it is foreseeable that ETCs will be more profitable than FPCs, but only under the LPG subsidy removal scenario.

When we analyse the energy requirements of backup systems powered by electricity, we also consider two different scenarios: subsidized electricity and unsubsidized electricity. The results

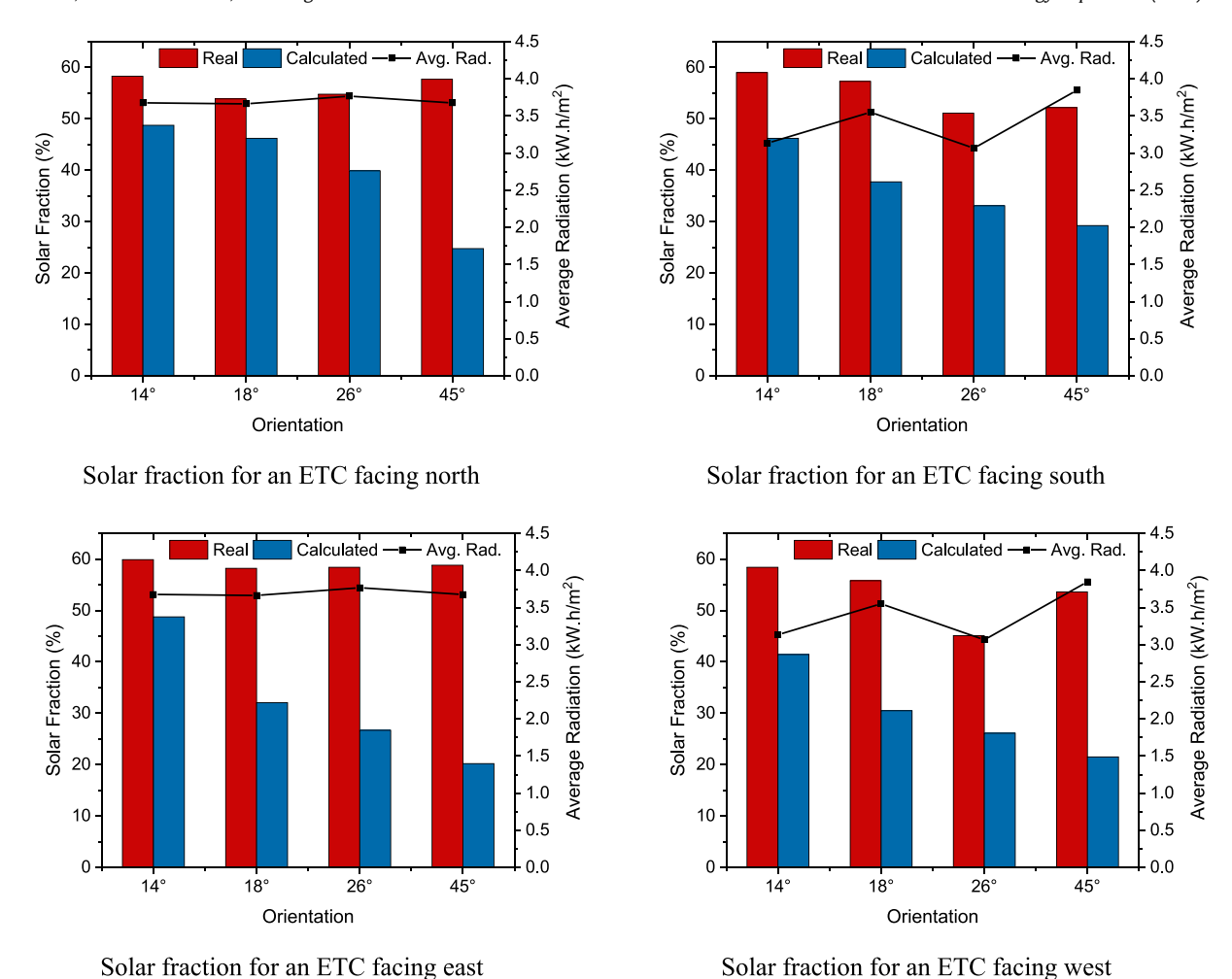


Fig. 4. Real vs. calculated solar fraction - ETC and average radiation.

Table 6Unmet energy requirement - ETCs.

ST collector inclination and orientation	Average monthly unmet energy requirement (kWh)	15 kg LPG tank units required	\$ in LPG per month (at subsidized value)	\$ in LPG per month without subsidy (\$23.03 per cylinder as of May 2, 2022)	\$ in electricity per month (at subsidized value, \$0.10)	\$ in electricity per month (without subsidy \$0.1559)
14° west	158.894	0.792	1.34	18.24	15.88	24.77
18° west	165.287	0.824	1.40	18.97	16.52	25.77
26° west	189.476	0.944	1.60	21.75	18.94	29.54
45° west	185.003	0.922	1.56	21.23	18.50	28.84
14° east	161.574	0.805	1.36	18.54	16.15	25.19
18° east	161.476	0.805	1.36	18.53	16.14	25.17
26° east	162.927	0.812	1.38	18.70	16.29	25.40
45° east	158.894	0.792	1.34	18.24	15.88	24.77
14° south	160.931	0.802	1.36	18.47	16.09	25.09
18° south	171.248	0.854	1.45	19.65	17.12	26.70
26° south	212.811	1.061	1.80	24.42	21.28	33.18
45° south	179.739	0.896	1.52	20.63	17.97	28.02
14° north	155.234	0.774	1.31	17.81	15.52	24.20
18° north	159.905	0.797	1.35	18.35	15.99	24.93
26° north	161.258	0.804	1.36	18.51	16.12	25.14
45° north	159.570	0.795	1.35	18.31	15.95	24.88
Average per mon	th		1.42	19.39	16.89	26.35

are presented in Tables 5 and 6. With subsidized electricity, the monthly minimum expenditure established for systems powered with FPCs for backup electricity is US\$19.27, and the maximum is US\$25.13. In the case of installations supplied by ETCs, the minimum monthly expenditure is \$15.88 USD, and the maximum is US\$21.28. The average spending for subsidized electricity in

the cases analysed is US\$20.72 for FPC technology and US\$16.89 for ETC technology. This finding implies that over the 15-year useful life of the equipment, the foreseeable savings are approximately US\$689.04. This value is somewhat lower than that determined for the water heating scenario with unsubsidized LPG. Consequently, with subsidized electricity, the advisability of

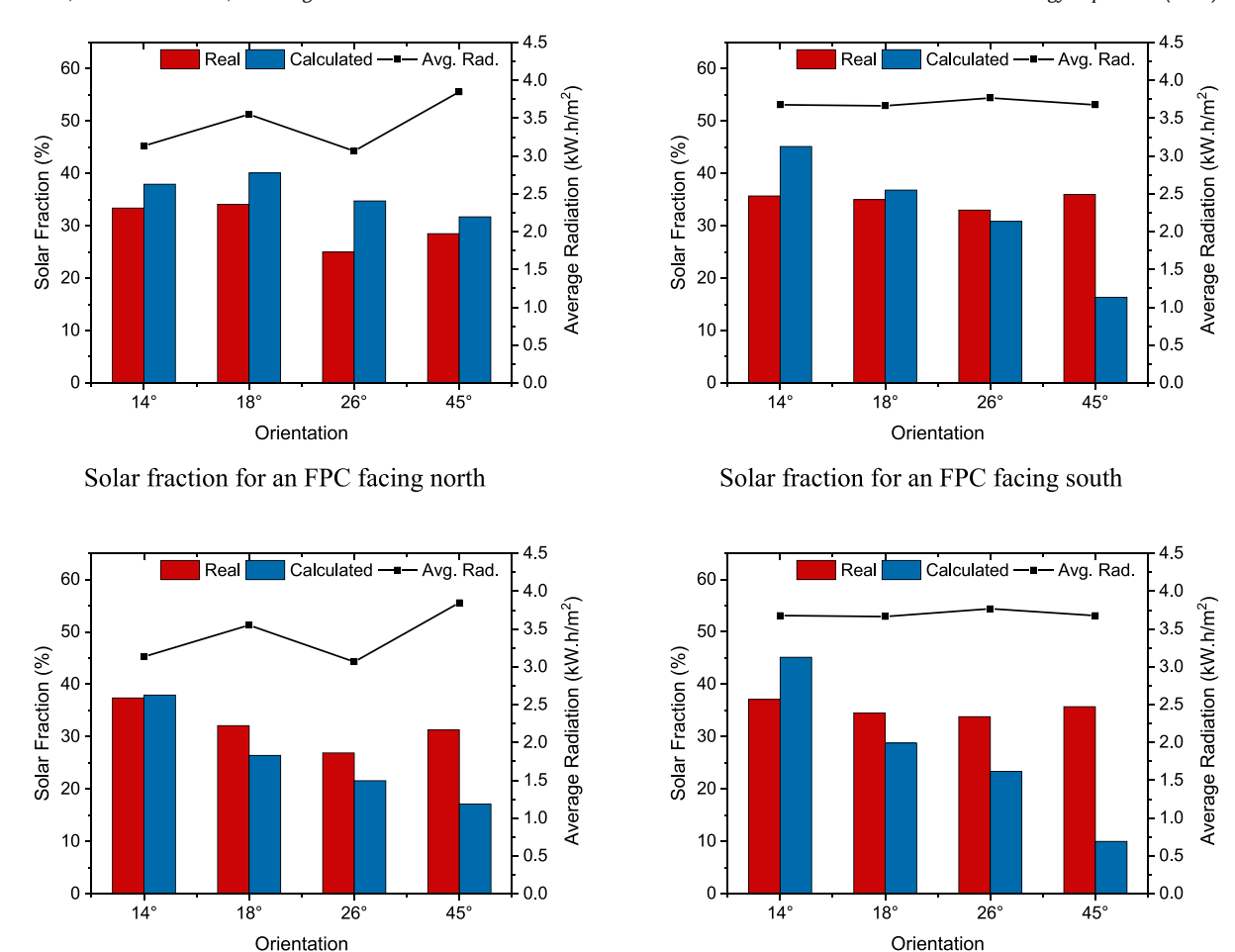


Fig. 5. Real solar fraction f_{real} vs. calculated solar fraction f_{cal} – FPC.

one technology over the other for the future is not clear; it will depend on the future cost of electricity, although due to recent trends, it is foreseeable that both would be slightly more advisable. Finally, for the scenario of electricity without the subsidy, we establish that for installations powered by FPC technology, a minimum of US\$30.05 and a maximum of US\$39.18 of monthly nonsubsidy electricity supplying backup water heating is required to reach 50 °C, with the average of the cases analysed being US\$32.30; for ETC technology, it would be necessary to spend a maximum of US\$33.18 and a minimum of US\$24.20 monthly, with the average required economic expenditure being US\$26.35 for electricity. This result suggests that based on the two technologies and power as a backup for unsubsidized electricity, in a 15-year period, the cost difference between the two technologies in electricity would be US\$1071.00. This difference is greater than the installation cost difference between the technologies, which is estimated at US\$537.50. The comparative analyses clearly indicate that the higher the cost of backup power is, the more beneficial ETC technology becomes.

Solar fraction for an FPC facing east

4. Discussion and conclusions

Compared to the results obtained by studies of ST systems for DHW in different contexts and in the same context as this study, our obtained results are unique in terms of the proposed method and the parameters analysed and modified for interpreting the performance and potential of ST systems. In our literature review, no validation studies were found that built systems to simulate

residential consumption; determined the efficiency of the two technologies integrated into ST systems, including storage, fluid networks, and pumping, with collectors for each of the two ST technologies deployed in different inclination and orientation configurations; or considered hot water discharges in accordance with the potential residential use of four inhabitants. The solar capacities of the FPC and ETC technologies were already comparatively analysed in several previous studies, in which the reliability of the F-chart model was determined using dynamic tools, finding similar results with a lag of only 5% (Dongellini et al., 2015). However, Han and others (Han et al., 2010) determined that the recommended implementation of FPCs in the province of Zhejiang in China, which has low-irradiance conditions compared to the remaining country, is more financially feasible than the implementation of ETCs, although the latter technology is supposed to be more efficient under diffuse solar irradiance. The difference lies in the cost of the technologies, which coincides with the results obtained in this study when the backup energy sources are subsidized.

Solar fraction for an FPC facing west

The purchase and installation process of complete solar thermal systems was also evaluated. For FPC technology, the cost is approximately US\$887.50, compared to the US\$1425.00 cost of the ETC system in Ecuador. The cost difference lies mainly in the collectors and minimally in the storage (200 L versus 300 L). Storage capacity is provided by kits from local sellers, although reference studies suggest that 200 L are optimal for residential use but that 300 litre capacities do not reduce the capacity of ST systems and may instead may slightly improve the solar

fraction when consumption is high (Żelazna and Gołębiowska, 2022). Although the thermal loss coefficient of ETCs is initially approximately a quarter compared with FPCs, this parameter is decisive when the ambient temperature is low for FPCs, ETCs are more fragile during transportation, handling and assembly, as their glazing is typically weaker (Duffie, 1986). Comparing the performance of the technologies, in winter months, ETCs are up to three times more efficient than FPCs; however, in terms of annual balance, their advantage is significantly weakened to approximately 12% in the seasonal climate of Brasov, Romania (Moldovan et al., 2020). A previous study in Cuenca carried out with the same equipment as that used in this study demonstrated that ETCs can reach an efficiency that implies up to 20.6% less backup energy compared to FPCs when the collectors are deployed almost horizontally. Furthermore, ETCs are affected by the incidence of shadows between tubes, which does not affect FPC technology (Zalamea-Leon et al., 2021).

Comparing f_{real} with f_{cal} of the simulated model through the F-chart model, differences between the ST technologies are observed. On average, in the four analysed inclinations representing different roof slopes (14°, 18°, 26° and 45°) and in the four cardinal orientations, the average value of f_{real} for the ETCs over the 16 cases is 55.99, while the indicator f_{cal} only reaches 34.16. This finding indicates that for ETC technology, in general, the Fchart model presents a significant dispersion and difference with respect to the real performance, and the performance of the ETCs is more efficient than that indicated by the simulation results. Similarly, for ETCs, the reduced performance due to orientation and inclination is lower for f_{real} than for f_{cal} , and the observed variability is a consequence of the irradiance levels, being substantially higher under intense direct solar irradiance (over 3.55 kWh/m² day). f_{real} reaches 55.6 with a collector inclination of 45°. However, with an average solar irradiance of less than 3.1 kWh/m² day, it does not exceed 52.4. The FPCs perform similarly in the real performance than in the simulated performance, although f_{cal} slightly exceeds f_{real} , with an average reading over all analysed orientations and inclinations for the FPCs of 33.09 for f_{real} compared to 30.25 for f_{cal} . Similar to the trend observed for the ETCs, under low solar irradiance conditions, the solar fraction is the lowest obtained when comparing all the cases, despite not being in a maximum inclination arrangement as expected. Additionally, for the FPCs, f_{real} decreases as the inclination increases, as expected; thus, taking the average f_{real} when the collectors are inclined at 14° yields a fraction of 35.90 compared to the average freal value of 32.88 over the four orientations at a measured inclination of 45° . f_{cal} significantly decreases from 41.55 averaged over the four orientations to 18.79 at 45°. This finding assumes that f_{cal} attains very optimistic average values at smaller inclines and very unfavourable average values at steep inclines. The general trend indicates that in most cases, the use of the F-chart model is pessimistic for the two technologies. However, this may change, for example, in the scenario of long runs and losses in hydraulic networks that depend on the building size and extension. Losses can be more significant, but the F-chart model does not consider any parameter that determines losses by network extensions or the quality of their isolation. Another aspect that is important and that the F-chart model does not consider is the losses caused by not using the obtained energy for long periods or simply by lower DHW consumption, which implies significant losses in general, as Guilló et al. analysed (Guilló et al., 2008). Based on the established differences, it is concluded that the F-chart model is unreliable, as when parameterizing the different variables in the most similar possible way, even climatic variables, the obtained results mostly differed substantially from the real behaviour, as reflected in Tables 3 and 4.

Finally, an economic analysis was conducted, considering only f_{real} for the two technologies. For the sanitary DHW flows established in Table 1, the unmet energy required to reach a temperature of 50 °C was regarded as the demanded temperature. Four scenarios were compared: replacement systems powered with subsidized LPG, LPG at cost without a subsidy, electricity with the current subsidies prices and electricity without a subsidy. By taking the average performance of all the measurements carried out over seven months in the local climate, it was determined that ETC technology is 18.5% more efficient in terms of the solar fraction. However, due to the higher technological cost and greater storage capacity of an ETC facility, it is determined that with the current subsidized LPG price, FPC technology is more attractive, whereas with the current LPG price, the introduction of the technology in Ecuador is unfeasible. In the case of unsubsidized LPG and subsidized electricity, the better performance of ETC technology makes up for its higher cost. Finally, in the case of powering with electricity at a real price, ETC technology is slightly more advantageous.

This research has shown the expected deviation of the real performance of ST and a comparison of technologies. Further research should be performed since it is necessary to determine the main parameters and the extent to which they affect and deviate from the existing models with the real performance of a residential ST system. Additionally, local climate and residential customers for hot water use influence real performance. Overall, background research has been performed on ST collectors' efficiency or storage as individual aspects, mainly from simulating in concordance with energy availability or demands to solve. However, for residential ST in integrated systems, the deviation has been demonstrated to be high. Several aspects must be accounted for, such as the storage limitations and losses, losses expected on hot water distribution pipes and flows, and the time of thermal consumption. In addition to other nonresidential uses, this kind of real performance should also be important.

CRediT authorship contribution statement

Esteban Zalamea-León: Conceptualization, Data curation, Formal analysis, Funding acquisition, Investigation, Methodology, Project administration, Resources, Supervision, Visualization, Writing – original draft. **Mateo Astudillo-Flores:** Data curation, Investigation, Project administration, Software, Visualization, Writing – original draft. **Antonio Barragán-Escandón:** Conceptualization, Funding acquisition, Validation, Writing – review & editing. **Manuel Raúl Peláez-Samaniego:** Methodology, Supervision, Validation, Writing – review & editing.

Declaration of competing interest

The authors declare that they have no known competing financial interests or personal relationships that could have appeared to influence the work reported in this paper.

Data availability

Data will be made available on request.

Acknowledgements

This document expresses results obtained with and research performed with the support of the Vicerrectorado de Investigación de la Universidad de Cuenca and Virtualtech Research Group, as well as the *Grupo de Investigación en Energía of the Universidad Politécnica Salesiana*. This work is a result of the "Modelado y mediciones de condiciones ambientales interiores e integración de energía solar, para alcanzar el Estándar Net-Zero en Edificaciones FAUC" Research Project.

Appendix A. Supplementary data

Supplementary material related to this article can be found online at https://doi.org/10.1016/j.egyr.2023.09.072. This document expresses results obtained with and research performed with the support of the Vicerrectorado de Investigación de la Universidad de Cuenca and Virtualtech Research Group, as well as the Grupo de Investigación en Energía of the Universidad Politécnica Salesiana. This work is a result of the "Modelado y mediciones de condiciones ambientales interiores e integración de energía solar, para alcanzar el Estándar Net-Zero en Edificaciones FAUC" Research Project.

References

- Agencia de Regulación y Control de la Electricidad, 2022. Informe Técnico Económico Para El anáLisis Y Determinación Del Costo Total Del Sector Eléctrico. QUITO.
- Apricus, 2021. ETC-20 solar collector [www document]. URL https: //www.apricus.com/en/america/products/solar-collectors/ap-20/index.html (accessed 1.9.22).
- APS Products, 2020. Separated pressure solar water heater [www document]. URL http://www.aps-china.net/aps/ArticleShow1.asp?ArticleID=4697 (accessed 12.13.21).
- Astrov, V., Grieveson, R., Kochnev, A., Landesmann, M., Pindyuk, O., 2022. Possible Russian invasion of Ukraine, scenarios for sanctions, and likely economic impact on Russia, Ukraine and the EU.
- Astudillo-flores, M., Zalamea-leon, E., Barragán-escandón, A., Pelaez-Samaniego, M.R., Calle-siguencia, J., 2021. Modelling of solar thermal energy for household use in equatorial latitude by using the F-chart model. In: ICREPO 21.
- Autonic, 2021. Autonic serie TM [www document]. URL https://www.autonics. com/series/3000413 (accessed 12.13.21).
- Bari, S., 2000. Optimum slope angle and orientation of solar collectors for different periods of possible utilization. Energy Convers. Manag. 41, 855–860. http://dx.doi.org/10.1016/S0196-8904(99)00154-5.
- Beckman, W.A., Klein, Sanford A., Duffie, J.A., 1977. Solar heating design, by the f-chart method [www document].
- Calle-Siguencia, J., Tinoco-Gómez, Ó., 2018. Obtención de ACS con energía solar en el cantón cuenca y análisis de la contaminación ambiental obtaining of SHW with solar energy in the canton cuenca and analysis of environmental pollution. Ingenius 89–101. http://dx.doi.org/10.17163/ings.n19.2018.09.
- Creamer-Guillen, B., Becerra-Robalino, R., 2016. Cuantificación de los subsidios de derivados del petróleo a los hidrocarburos en el ecuador. Bol. Estad. Sect. Hidrocarb. 2, 9–26.
- Delta-T devices, 2019. WS-GP2 advanced automatic weather station system [www document]. URL https://www.delta-t.co.uk/product/ws-gp2/ (accessed 3.4.19).
- Dongellini, M., Falcioni, S., Morini, G.L., 2015. Dynamic simulation of solar thermal collectors for domestic hot water production. Energy Procedia 82, 630–636. http://dx.doi.org/10.1016/j.egypro.2015.12.012.
- Duffie, J.A., 1986. Solar technologies. In: Twidell, J., Hounam, I., Lewis, C. (Eds.), Energy for Rural and Island Communities IV. Proc. 4th International Conference, Inverness, 1985. Pergamon Books Ltd, pp. 275–280. http://dx.doi.org/10.1016/B978-0-08-033423-3.50042-3.
- Gajbert, H., 2008. Solar Thermal Energy Systems for Building Integration. Lund University.
- Guilló, J.F., Lucas, M., Lucas, R., Vicente, P.G., 2008. CáLculo de la Contribución Solar Térmica En Instalaciones de Acs. Universidad de Vigo, Vigo.
- Han, J., Mol, A.P.J., Lu, Y., 2010. Solar water heaters in China: A new day dawning. Energy Policy 38, 383–391. http://dx.doi.org/10.1016/j.enpol.2009.09.029.
- Hetzonneboilerhuis, 2015. Operation manual of solar controller SR658for split solar system.
- IEA, SHC, 2022. IEA solar heating & cooling programme [www document]. URL https://www.iea-shc.org/tasks (accessed 11.21.22).
- International Renewable Energy Agency (IRENA), 2021. Sector coupling in facilitating integration of variable renewable energy in cities.
- IRENA, ILO, 2021. Renewable Energy and Jobs Annual Review 2021. Abu Dhabi.

- Izquierdo-torres, I.F., Pacheco-portilla, M.G., Gonzalez-Morales, L.G., Zalamea-Leon, E.F., 2019. Photovoltaic simulation considering building integration parameters. INGENIUS Rev. Cienc. Tecnol. 21, 9–19. http://dx.doi.org/10. 17163/ings.n21.2019.02.
- Kalogirou, S.a., 2004. Solar thermal collectors and applications. Prog. Energy Combust. Sci. 30, 231–295. http://dx.doi.org/10.1016/j.pecs.2004.02.001.
- Klein, S.A., Beckman, W.A., Duffie, J.A., 1976. A design procedure for solar heating systems. Sol. Energy 18, 113–127. http://dx.doi.org/10.1016/0038-092X(76)90044-X.
- Minenergia, 2022. Sistemas solares termicos [www document]. URL https://sst.minenergia.cl/?page_id=268.
- Ministerio de Desarrollo Urbano y Vivienda, 2020. NEC-HS-ER, Sistemas Solares Térmicos Para Agua Caliente Sanitaria (ACS) – Aplicaciones Menores a 100 ° C. Quito, Ecuador.
- Moldovan, M., Visa, I., Burduhos, B., 2020. Experimental comparison of flat plate and evacuated tube solar thermal collectors for domestic hot water preparation in education facilities. J. Sustain. Dev. Energy Water Environ. Syst. 8, 293–303. http://dx.doi.org/10.13044/j.sdewes.d7.0285.
- Morse, E.S., 1881. Warming and ventilating apartments by the sun's rays. Specification 246, 626.
- Mulcué-Nieto, L.F., Mora-López, L., 2017. A novel methodology for the preclassification of façades usable for the decision of installation of integrated PV in buildings: The case for equatorial countries. Energy 141, 2264–2276. http://dx.doi.org/10.1016/j.energy.2017.11.150.
- Munari, C., 2009. Architectural Integration and Design of Solar Thermal Systems. École Polytechnique Fédérale de Jausanne.
- Obaco, F., Jaramillo, J., 2010. Sistemas solar-térmicos: algoritmo operativo para aplicar el método F- chart en la evaluación de colectores solares. pp. 1–3.
- Okafor, I.F., Akubue, G., 2012. F-chart method for designing solar thermal water heating systems. Int. J. Sci. Eng. Res. 3, 1–7.
- Perez, R., Perez, M., 2009. A fundamental look at energy reserves for the planet. Int. Energy Agency SHC Program. Sol. Updat. 50, 4–6.
- Petroprices, G., 2022. Precio del autogas, galon, 13 de junio del 2022 [www document]. URL https://es.globalpetrolprices.com/lpg_prices/#hl37.
- Prapas, D.E., Norton, B., Milonidis, E., Probert, S.D., 1988. Response function for solar-energy collectors. Sol. Energy 40, 371–383. http://dx.doi.org/10.1016/ 0038-092X(88)90010-2.
- Recalde, C., Cisneros, C., Avila, C., Logroño, W., Recalde, M., 2015. Single phase natural circulation flow through solar evacuated tubes collectors on the equatorial zone. Energy Procedia 75, 467–472. http://dx.doi.org/10.1016/j. egypro.2015.07.424.
- Shah, L.J., Furbo, S., 2004. Vertical evacuated tubular-collectors utilizing solar radiation from all directions. Appl. Energy 78, 371–395. http://dx.doi.org/10. 1016/j.apenergy.2003.10.004.
- Singh, G., Das, R., 2021. Experimental study of a combined biomass and solar energy-based fully grid-independent air-conditioning system. Clean Technol. Environ. Policy 23, 1889–1912. http://dx.doi.org/10.1007/s10098-021-02081-
- Singh, G., Das, R., 2022. A novel variable refrigerant flow system with solar regeneration-based desiccant-assisted ventilation. Sol. Energy 238, 84–104. http://dx.doi.org/10.1016/j.solener.2022.04.008.
- The World Counts, 2023. Global energy consumption [www document].
- United Nations, Department of Economic and Social Affairs, P.D., 2018. The world 's cities in 2018, the world's cities in 2018 data booklet (ST/ESA/ ser.a/417). Vázquez, Espí. M., 1999. Una prevísima historia de la arquitectura solar. Por
- Vázquez Espí, M., 1999. Una brevísima historia de la arquitectura solar. Por Arquit. Urban Contemp. 1–31.
- Weiss, W., Spörk-Dür, M., 2019. Solar heat worldwide 2020 global market development and trends in 2019. Sci. Technol. Built Environ..
- Zalamea-Leon, E., Barragan, E., Calle-Sigüencia, J., Astudillo-Flores, M., Juela-Quintuña, D., 2021. Residential solar thermal performance considering self-shading incidence between tubes in evacuated tube and flat plate collectors. Sustainability 13, http://dx.doi.org/10.3390/su132413870.
- Zalamea-león, E., Barragán-escandón, A., 2021. Arquitectura, Sol Y Energía, first ed. Ucuenca Press, Cuenca.
- Zambolin, E., Del Col, D., 2010. Experimental analysis of thermal performance of flat plate and evacuated tube solar collectors in stationary standard and daily conditions. Sol. Energy 84, 1382–1396. http://dx.doi.org/10.1016/j.solener. 2010.04.020.
- Żelazna, A., Gołębiowska, J., 2022. Designing for the environment: An example of multi-criteria analysis used for solar hot water system selection. Energies 15, http://dx.doi.org/10.3390/en15010065.
- Zhang, T., Zheng, W., Wang, L., Yan, Z., Hu, M., 2021. Experimental study and numerical validation on the effect of inclination angle to the thermal performance of solar heat pipe photovoltaic/thermal system. Energy 223, 120020. http://dx.doi.org/10.1016/j.energy.2021.120020.